Japanese Journal of Applied Physics

The Japan Society of Applied Physics

ACCEPTED MANUSCRIPT

Low-frequency sound absorbing metasurface using multilayer split resonators

To cite this article before publication: Shota Takasugi *et al* 2021 *Jpn. J. Appl. Phys.* in press https://doi.org/10.35848/1347-4065/abe2e5

Low-frequency sound absorbing metasurface using multilayer split resonators

Shota Takasugi, Keita Watanabe, Masaaki Misawa, and Kenji Tsuruta*

Department of Electrical and Electronic Engineering, Okayama University

3-1-1 Tsushima-naka, Kita-ku, Okayama 700-8530, Japan

Among the acoustic metasurfaces that can control the propagation of sound waves with the structure far thinner than the wavelength at the operating frequency, the split tube structure has shown its effectiveness in the lower frequency band. Here we focus on multiply layered split tubes to broaden the absorption spectrum. By numerical analysis, we show up-to six-layer structure possessing wideband (1 to 1000 Hz) sound absorption. The absorbing peaks in the frequency band below 1000 Hz are shown to be multiplexed not only by simple superposition of vibrational modes of each layer, but also by hybridization of the modes indicating collective motion of tubes.

*E-mail: tsuruta@okayama-u.ac.jp

ORCID
Kenji Tsuruta: 0000-0002-1447-2530

1. Introduction

Sound absorption/insulation technology has always been required in many places such as houses and public facilities. Low-frequency sounds are not only harmful to objects, but also to mental health such as oppressive feeling and discomfort, and hence countermeasures are necessary. In the environment that requires high sound absorption/insulation performance, thick and heavy sound absorbing materials[1-3] have often been used despite their cost fullness. It has thus been desired to develop a new class of materials that can absorb/shield the low-frequency sound without the heavy mass and large thickness.

In previous research, we have been focusing on the Decorated Membrane Resonator (DMR) [4-6], which is one of the acoustic metasurfaces [7-11]. Metasurface in general is an artificial structure based on a build-in resonator that localizes strongly oscillating fields on the surface at certain frequencies and hence it can control/modulate the incident waves despite of its characteristic thickness well below wavelength of the waves. As for acoustic applications, metasurface has shown novel properties; acoustic cloaking,[12-14] complete sound transmission[15,16] /reflection[17,18]/ absorption,[19-22] and wave-front tailoring.[23] It has been shown that the DMR can achieve nearly 100% sound absorption at the resonance frequency. However, it is difficult to achieve the efficiency in low-frequency range below 1000Hz by the metasurface unless the size of the resonator is large enough. Other metasurfaces than DMR, such as a three-dimensional single-port labyrinthine structure[24] and split tube resonators[25,26], have been proposed to overcome this drawback. Those structures have the sharp peak at the resonant frequency hampering to utilize the structure in practical applications in ambient sound environments with relatively wide frequency spectra. In the present study, we propose a device that can absorb and block low-frequency sound over a wide range by multiplexing split tube resonators.

2. Acoustic absorber based on split tube resonators

The low-frequency tunable acoustic absorber based on split tube resonators originally proposed in Ref. 4 is a polylactide (PLA) elliptic cylinder with a side cut so that the cross section becomes a split ring. Here the base structure was designed with polylactide (PLA) in order to reduce the total weight of the structure. The aluminum plate has the role of reflecting sound waves which resonate with the sound absorber, as well as the role of preventing sound

transmission. Figure 1(a) shows the basic structure of a split tube, and Figure 1(c) shows its sound absorption coefficient. The wavelength of the sound wave at 516 Hz, at which the sound absorption peak in Fig. 1(b) was obtained, was about 66 cm, whereas the thickness of the sound absorbing structure including the split tube and the aluminum plate was 2.5 cm. The high sound absorption characteristics are thereby exhibited even in low-frequency sounds where sound absorption is difficult due to the long wavelength. The principle of absorbing sound is based on conversion of the sound energy into heat energy by mutual vibration of the split tube and the air layer [27-29]. In the current FEM simulation, the viscosity of air is also considered, but the loss of polylactide accounts for the majority. Despite that it achieves nearly 100% sound absorption at the resonant frequency, the sharp peak at the resonant frequency hampers to utilize the structure in practical applications that have ambient sound environments with relatively wide frequency spectra[30].

3. Multilayer split tube structure

3.1 Analysis model

To solve the problem of narrow frequency band, we focus on multiplexing the split tubes with different size to broaden the absorption spectrum. In this analysis, the number of layers of the tube was changed from two through six. Considering that the original design has a structure in which the sound reflected from the aluminum plate penetrates into the hole of the outermost split tube, the hole of the outermost split tube is designed to be proximate to the aluminum plate side.

3.2 Simulation method

For the acoustic wave calculation, we used the software package COMSOL Multiphysics[31] based on the finite element method (FEM). The triangular mesh divisions in the FEM simulations were performed for the surfaces of the sample and then swept to the entire sample with the same polygon. The Young's modulus, Poisson's ratio, density, and isotropic loss factor of polylactide are set to be 1280×10^6 Pa, 0.36, 1.252 g/cm^3, 0.008, respectively. Density and sound velocity of air are 1.2053 kg/m^3 and 343m/s, respectively. In the present FEM simulation, the effect of the viscosity of air is neglected.

A plane wave of 1 Pa sound pressure was incident vertically from the top of the structure. In the analysis, the total system is assumed to be surrounded by a rectangular parallelepiped

hard wall with the same radius as the sample in order to emulate the absorption measurement performed in a rectangular parallelepiped pipe. The frequency spectrum was calculated for 1 to 1000 Hz with a 1 Hz increment. To evaluate the absorption characteristics, we calculated the absorption coefficient based on the transfer-function method.[32,33] The sound absorption coefficient is given by the following formula.

$$Sound\ Absorption = \frac{sound\ power\ not\ reflected\ [\mathrm{W}]}{incident\ sound\ power\ [\mathrm{W}]}$$

The reflected sound pressure was measured at two points placed between the sound source and the structure. The first point is located 100 mm away from the center of the structure, whereas the second point is located 150 mm away from the center of the structure.

3.3 **Analysis results**

In this analysis, to confirm whether it is possible to widen the bandwidth by changing the number of split tubes, the innermost split tube structure of all structures was fixed with the dimensions shown in Fig. 1. Then, it was designed to add new split tubes around it at regular intervals. Figure 2 shows a graph comparing the sound absorption peaks of a doubly- to a sextuply layered split tube.

3.3.1 **Double-layer split tube**

As shown in Fig. 3, the created model consists of a structure that combines two elliptical split tubes with holes twisted by 180 °. As with the single split tube, the material of the structure is polylactic acid (PLA), and an aluminum plate is placed and fixed as shown in the figure separately from the split tube. Figure 2 shows that two sound absorption peaks appear near 287 Hz and around 493 Hz. The second absorption peak near 493 Hz is close to the sound absorption peak around 516 Hz obtained by the single split tube. In addition, one new sound absorption peak appeared around 287 Hz. Figure 4 shows the mode shape at the resonance frequency with each sound absorption peak. Among the resonance frequencies in the result, only the first split tube from the inside vibrates in the mode shape at 493 Hz, whereas at the low frequency of 287 Hz, only the second split tube from the inside vibrates. Thus, each mode is considered to be single mode.

3.3.2 **Triple-layer split tube**

The model for a triple(three)-layer structure is shown in Fig. 5. From Fig. 2, three sound absorption peaks were obtained near 186 Hz, 274 Hz, and 495 Hz in ascending order of the frequency. Figure 6 shows the mode shape at each resonance frequency. It is evident in the figure that the resonance mode at 495 Hz in Fig. 6(a) and that at 274 Hz in Fig.6(b) correspond to the single mode originated by the second and the third layer respectively. Thus, the two of sound-absorbing peaks excluding the newly obtained sound-absorbing peak at 186 Hz are the same as the results of the single and the double-layer split tube.

3.3.3 **Four-layer split tube**

The model for a quadruple(four)-layer structure is shown in Fig. 7. Six sound absorption peaks were obtained at 124 Hz, 174 Hz, 275 Hz, 495 Hz, 731 Hz, and 982 Hz. Figure 8 shows the mode shape at the peak frequency. It is evident in the figure that the resonance mode at 495 Hz in Fig. 8(c), 274 Hz in Fig. 8(d), 174 Hz in Fig. 8(e), and 124 Hz in Fig. 8(f) correspond to the single mode originated by the second, the third, and the fourth layer respectively. Thus, the three of sound-absorbing peaks excluding the newly obtained sound-absorbing peak at 124 Hz are the same as the results of the single, double and triple-layer split tube. As for the resonance frequency higher than 495 Hz, the mode shape at 731 Hz and 982 Hz resulted in hybrid modes in which all the split tubes vibrate to produce a sound absorbing peak.

3.3.4 **Five-layer split tube**

The model for a quintuple(five)-layer structure is shown in Fig. 9. From Fig. 2, seven sound absorption peaks were obtained at 86Hz, 117 Hz, 176 Hz, 275 Hz, 495 Hz, 716 Hz, and 910 Hz. Figure 10 shows the mode shape at the peak frequency. It is evident in the figure that the resonance mode at 495 Hz in Fig. 10(c), at 275 Hz in Fig. 10(d), 176 Hz in Fig. 10(e), 117 Hz in Fig. 10(f), and 86 Hz in Fig. 10(g) correspond to the single mode originated by the second, the third, the fourth, and the fifth layer respectively. Thus, the four of sound-absorbing peaks excluding the newly obtained sound-absorbing peak at 86Hz are the same as the results of the single, double, triple, and four-layer split tube. Focusing on the resonance frequency higher than 495 Hz, the mode shape at 716 Hz and 910 Hz resulted in hybrid modes in which all the split tubes vibrate to produce a sound absorbing peak. These two

sound absorption peaks could be confirmed at positions of almost the same resonance frequency as in the quadruply layered tube. In addition, the quintuple split tube has higher sound absorption characteristics at 716 Hz.

3.3.5 **Six-layer split tube**

The model for a sextuplex(six)-layer structure is shown in Fig. 11. From Fig. 2, nine sound absorption peaks were obtained at 61 Hz, 81 Hz, 117 Hz, 176 Hz, 275 Hz, 494 Hz, 514 Hz, 691 Hz, and 870 Hz. Figure 12 shows the mode shape at the peak frequencies. It is evident in the figure that the resonance mode at 494 Hz in Fig. 12(d), 275 Hz in Fig. 12(e), 176 Hz in Fig. 12(f), 117 Hz in Fig. 12(g), 81 Hz in Fig. 12(h), and 61 Hz in Fig. 12(i) correspond to the single mode originated by the second, third, fourth, fifth and sixth layer respectively. Thus, the five of sound-absorbing peaks excluding the newly obtained sound-absorbing peak at 61 Hz are the same as the results of the single, double, triple, four and five-layer split tube. As for the resonance frequencies higher than 494Hz, the mode shapes at 691 Hz and 870 Hz resulted in hybridized modes in which all the split tubes vibrate to produce a sound absorbing peak. Regarding the mode shape with a resonance frequency of 514 Hz, not all the split tubes are vibrating, but the first and fourth split tubes are vibrating, generating a partially hybridized mode.

3.4 **Discussion**

We attempted to multiplex the sound absorption peaks by stacking two or more split tubes. From the analysis results of each multiply layered tube, two types of sound absorption peaks were obtained: a single mode sound absorption peak in which each tube vibrates nearly independently, and a hybrid-mode sound absorption peak in which all the layers vibrate. From Fig. 2, when the number of split tubes is increased one by one from the double-layer split tubes, the sound absorption peaks in the single mode are newly appeared one by one to the low frequency side in the frequency band of about 495 Hz. In addition, in the frequency band on the high frequency side of about 495 Hz, two sound absorption peaks due to the hybrid modes were confirmed in the quadruply or more multiply layered tubes.

In the previous work on the split-tube resonator in Ref. 19 and 34, the main mechanism of the efficient sound absorption has been reported as a consequence of high friction losses due to the large differences between the air pressure in interlayer channels and that in the

innermost tube. On the other hand, the present analysis reveals that the high losses of acoustic energy in the multilayer split tube resonator can be attribute dominantly to the large displacement of PLA layer near the holes in the cases of single modes and to that of harmonic vibrations of tube as a whole in the cases of hybrid modes. The participation of different harmonic modes in the hybrid modes is illustrated as exaggerated views in the insets of Figs. 8(a), 8(b), 10(a), 10(b).

4. Conclusion

We have verified the sound absorption of a split tube in the frequency band below 1000 Hz and the multiplexing of sound absorption peaks created by superposing multiple split tubes. We succeeded in multiplexing sound absorption peaks in the frequency band below 1000 Hz. We further found the multiplexing is not only by simple superposition of each mode but also by hybridization of mode that exhibits a collective motion of the tubes. Especially in the six-layer split tube, nine sound absorption peaks emerged. The six of the peaks in the frequency range lower than 500 Hz were due to the single mode, whereas the three sound peaks on the higher frequency range than 500 Hz were generated as the hybrid modes. Also, the present analysis reveals that the high losses of acoustic energy in the multilayer split tube resonator can also be attribute to the large displacement of PLA layer near the holes.

Further optimization of the structure, *i.e.* the number of layers, the size, and aspect ratio of tubes, is necessary in order to realize broader and higher absorption spectra. Attempts for numerical optimization as well as experimental verifications for a prototype structure fabricated by a 3D printer are in progress.

Acknowledgments

This work was supported in part by the JSPS KAKENHI Grant Number 17K19035.

References

1) D.-Y. Maa, Int. J. Acoust. Vib. **12**, 3 (2007).
2) D.-Y. Maa, Sci. Sin. **18**, 55 (1975).
3) D.-Y. Maa, J. Acoust. Soc. Am. **104**, 2861 (1998).
4) G. Ma, M. Yang, S. Xian, Z. Yang and P. Sheng, Nature Mater. **13**, 873 (2014).
5) M. Fujita, K. Manabe, K. Tsuruta, T. Hada, and N. Yorozu, Proc. Symp. on Ultrasonic Electronics (USE2018) **39**, 3P1-3 (2018).
6) K. Watanabe, M. Fujita and K. Tsuruta, Jpn. J. App. Phys. 59, SKKA06 (2020).
7) M. Dubois, C. Shi, Y. Wang and X. Zhang, Appl. Phys. Lett **110** 151902 (2017).
8) S. Xia, G. Ma, Y. Li, Z. Yang and P. Sheng, Appl. Phys. Lett **106**, 091904 (2015).
9) M. Khorasaninejad, F. Aieta, P. Kanhaiya, M. A. Kats, P. Genevet, D. Rousso and F. Capasso, Nano Lett. **15**, 5358 (2015).
10) J. Zhan, B. Li, Z. N. Chen and Cheng-Wei Qiu, Appl. Phys. Lett. **103**, 151604 (2013).
11) B. Yuan, Y. Cheng and X. Liu, Appl. Phys. Express **8** 027301 (2015).
12) S. Zhang, C. Xia, and N. Fang, Phys. Rev. Lett. **106**, 024301 (2011).
13) M. Farhat, S. Guenneau, and S. Enoch, Phys. Rev. Lett. **103**, 024301 (2009).
14) N. Stenger, M. Wilhelm, and M. Wegener, Phys. Rev. Lett. **108**, 014301 (2012).
15) S. H. Lee, J. J. Park, K. J. B. Lee, O. B. Wright, and M. K. Jung, Phys. Rev. Lett. **110**, 244302 (2013).
16) R. Fleury, and A. Al*ù*, Phys. Rev. Lett. **111**, 055501 (2013).
17) G. Ma, M. Yang, Z. Yang, and P. Sheng, Appl. Phys. Lett. **103**, 011903 (2013).
18) Y. Li, X. Jiang, R. L. B. Liang, X. Zou, L. Yin, and J. Cheng, Phys. Rev. Appl. **2**, 064002 (2014).
19) X. Wu *et al*., Appl. Phys. Lett. **112**, 103505 (2018).
20) X. Cai, Q. Guo, G. Hu, and J. Yang, Appl. Phys. Lett. **102**, 121901 (2014).
21) C. R. Liu, J. H. Wu, K. Lu, Z. T. Zhao and Z. Haung, Appl. Acoust. **148**, 1 (2019).
22) C. Fu, X. Zhang, M. Yang, S. Xiao and Z. Yang, Appl. Phys. Lett. **110**, 021901 (2017).
23) K. Tang, C. Qiu, M. Ke, J. Lu, Y. Ye and Z. Liu, Sci. Rep. **4**, 6517 (2014).
24) C. Zhang and X. Hu, Phys. Rev. Appl. **6**, 064025 (2016).
25) X. Wu, C. Fu, X. L. Y. Meng, Y, Gao, J. Tian, L. Wang, Y. Huang, Z. Yang and W. Wen, Appl. Phys. Lett. **109**, 043501 (2016).
26) S. Takasugi, K. Watanabe, M. Misawa and K. Tsuruta, Proc. Symp. on Ultrasonics

Electronics, Vol. 41, 3Pb1-1 (2020).

27) C. R. Liu, J. H. Wu, F. Ma, X, Chen and Z. Yang, Appl. Phys. Express **12** 084002 (2019).
28) D. Yang, X. Wang, and M. Zhu, J. Sound and Vibr. **333**, 6843 (2014).
29) Y. Kobayashi, K. Tsuruta, and A. Ishikawa, Proc. Symp. on Ultrasonic Electronics (USE2016) **37**, 3P1-2 (2016).
30) T. Sone, S. Kono, and T. Iwase *et al*., J. Acoust. Soc. Jpn. **50**, 233 (1994).
31) http://www.comsol.com
32) ISO 10534-2: 1998 "Acoustics – Determination of sound absorption coefficient and impedance in impedance tubes – Part2: Transfer-function method".
33) A. F. Seybert and D. F. Ross, J. Acoust. Soc. Am. **61**, 1362 (1977).
34) L. Jing, J.H.Wu, D. Guan, and N. Gao, J. Appl. Phys.**116**, 103514 (2014).

Figure

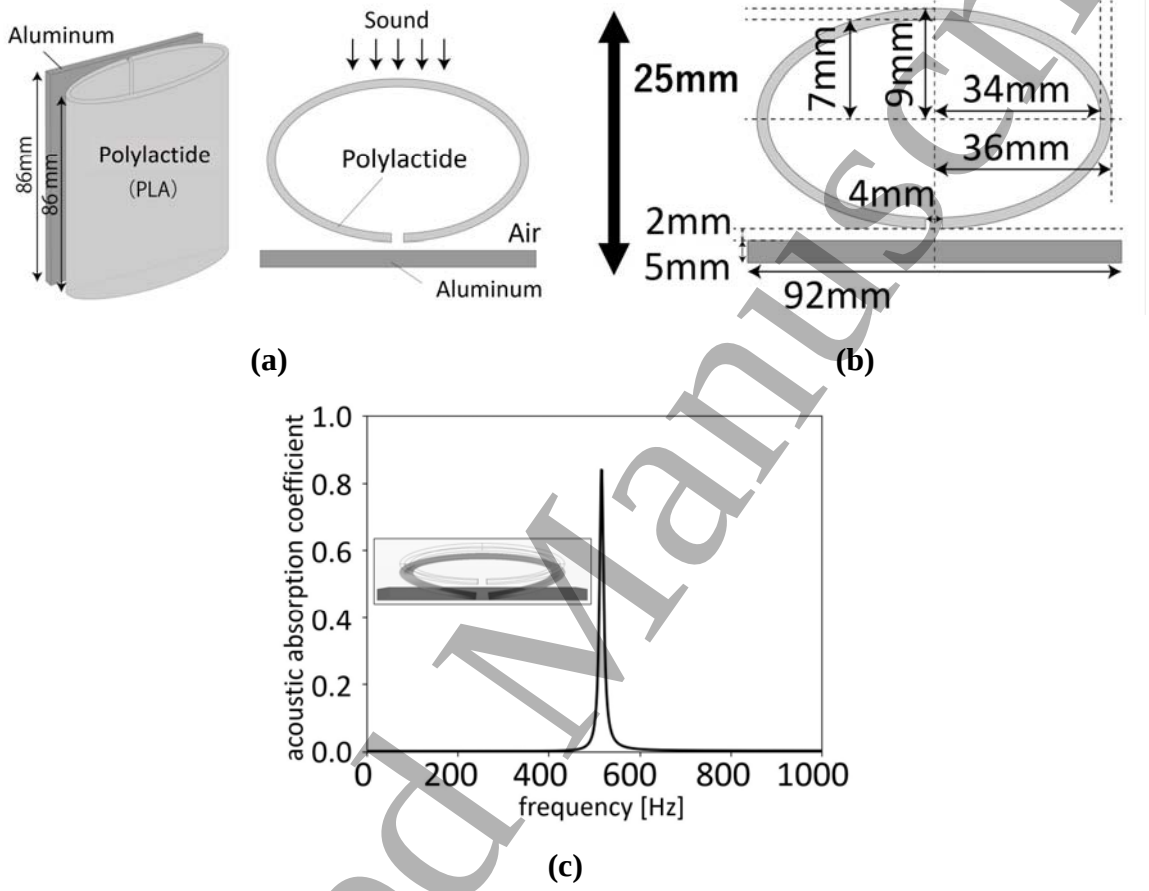

Figure 1 (a) The basic structure of a split tube, (b) its cross-sectional view, and (c) the sound absorption coefficient at the size of (b). A sharp absorption peak appears at about 516 Hz. The mode profile of a split tube at the peak frequency is shown in inset of (c).

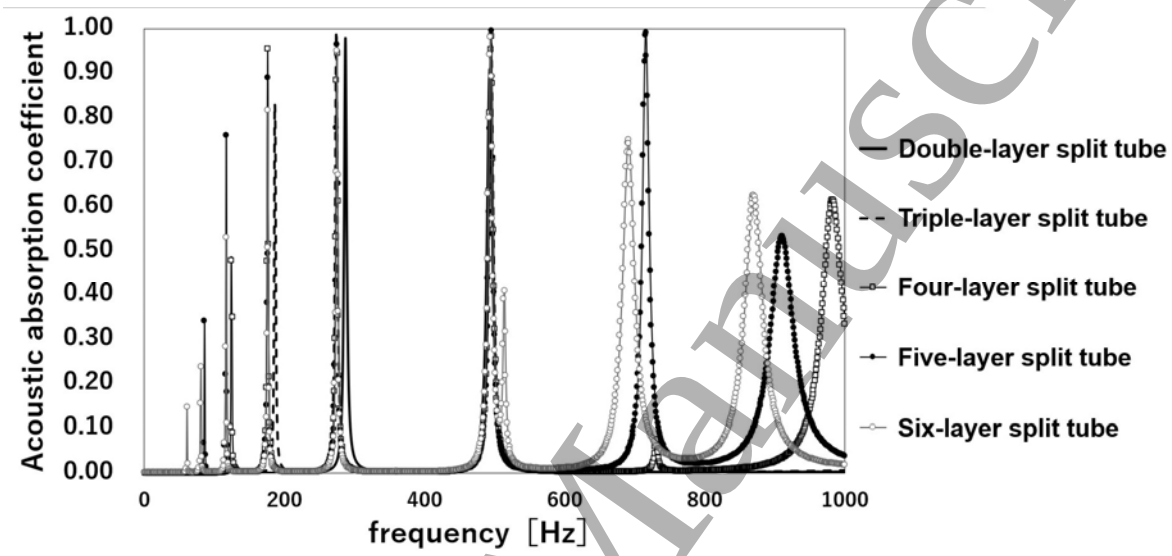

Figure 2 The sound absorption peaks of the double to six-layer split tubes.

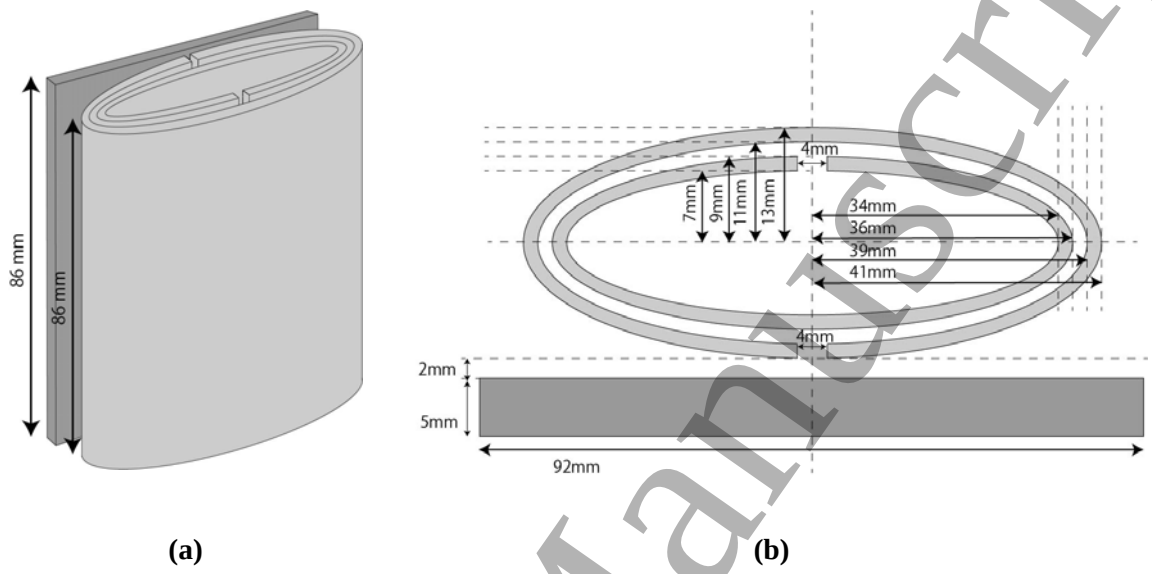

Figure 3 (a) The structure of a double-layer split tube and (b) its cross-sectional view.

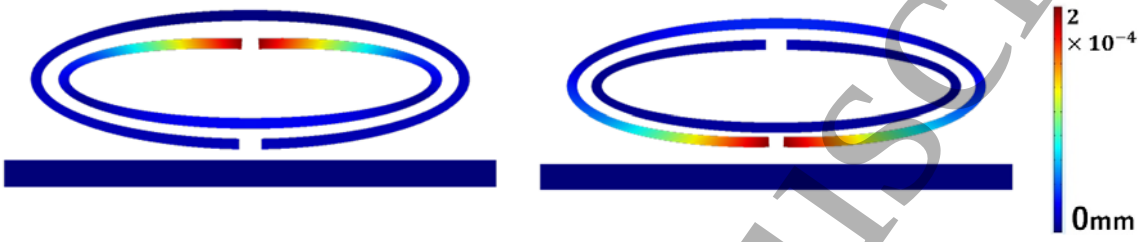

(a) 493 Hz (b) 287 Hz

Figure 4 The mode shape and displacement at (a) 493 Hz and (b) 287 Hz of the double-layer split tube. The color bar represents scales of the displacement norms drawn in the structure.

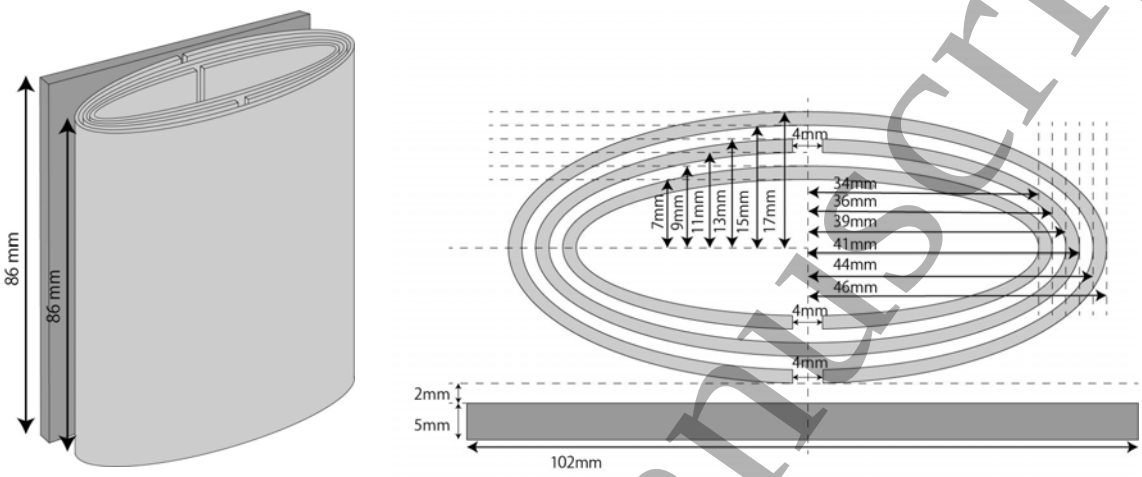

Figure 5 (a) The structure of a triple-layer split tube and (b) its cross-sectional view.

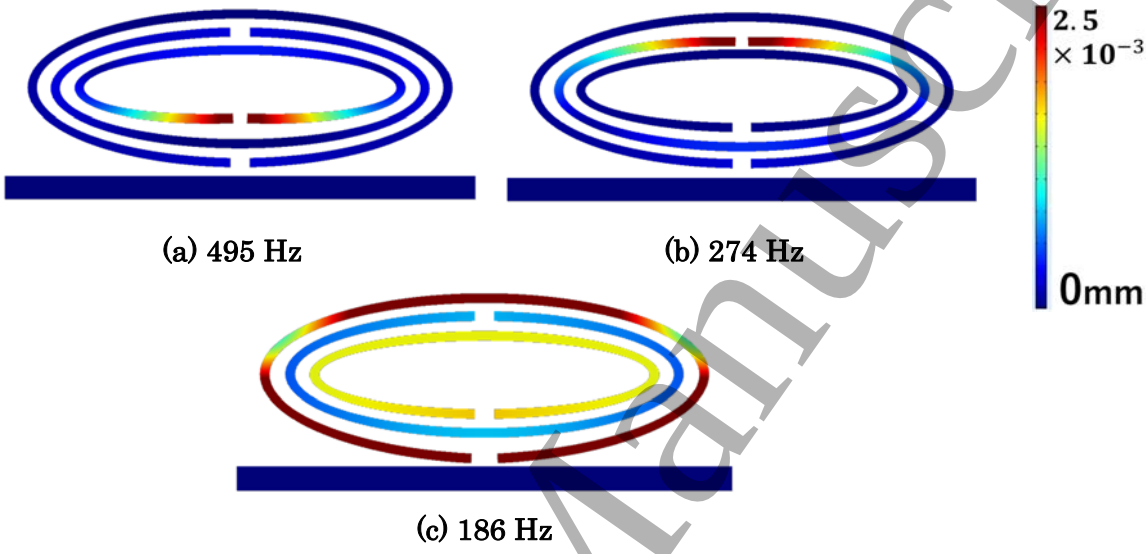

Figure 6 The mode shape and displacement at (a) 495 Hz, (b) 274 Hz, and (c) 186 Hz of the triple-layer split tube. The color bar represents scales of the displacement norms drawn in the structure.

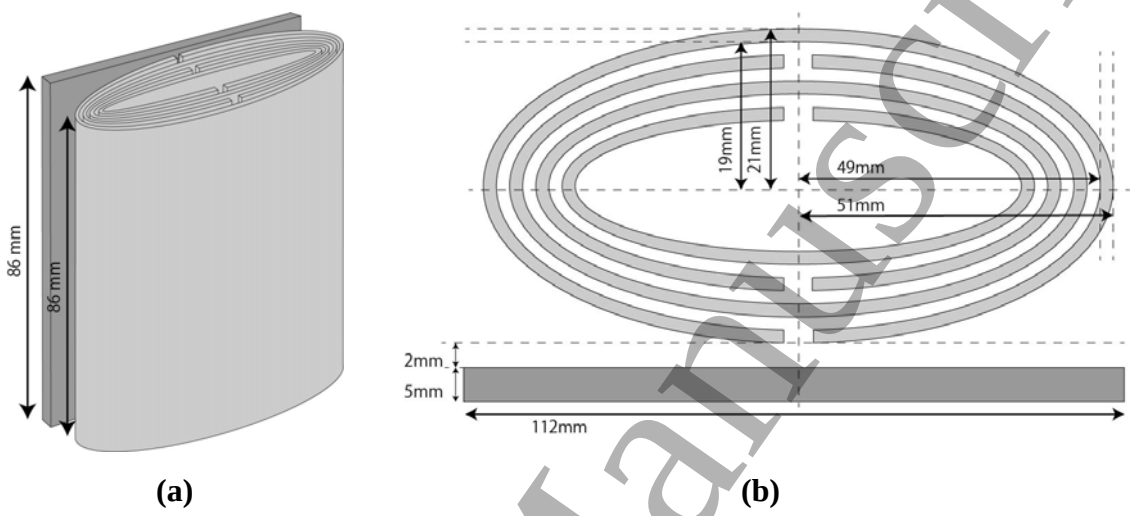

Figure 7 (a) The structure of a four-layer split tube and (b) its cross-sectional view.

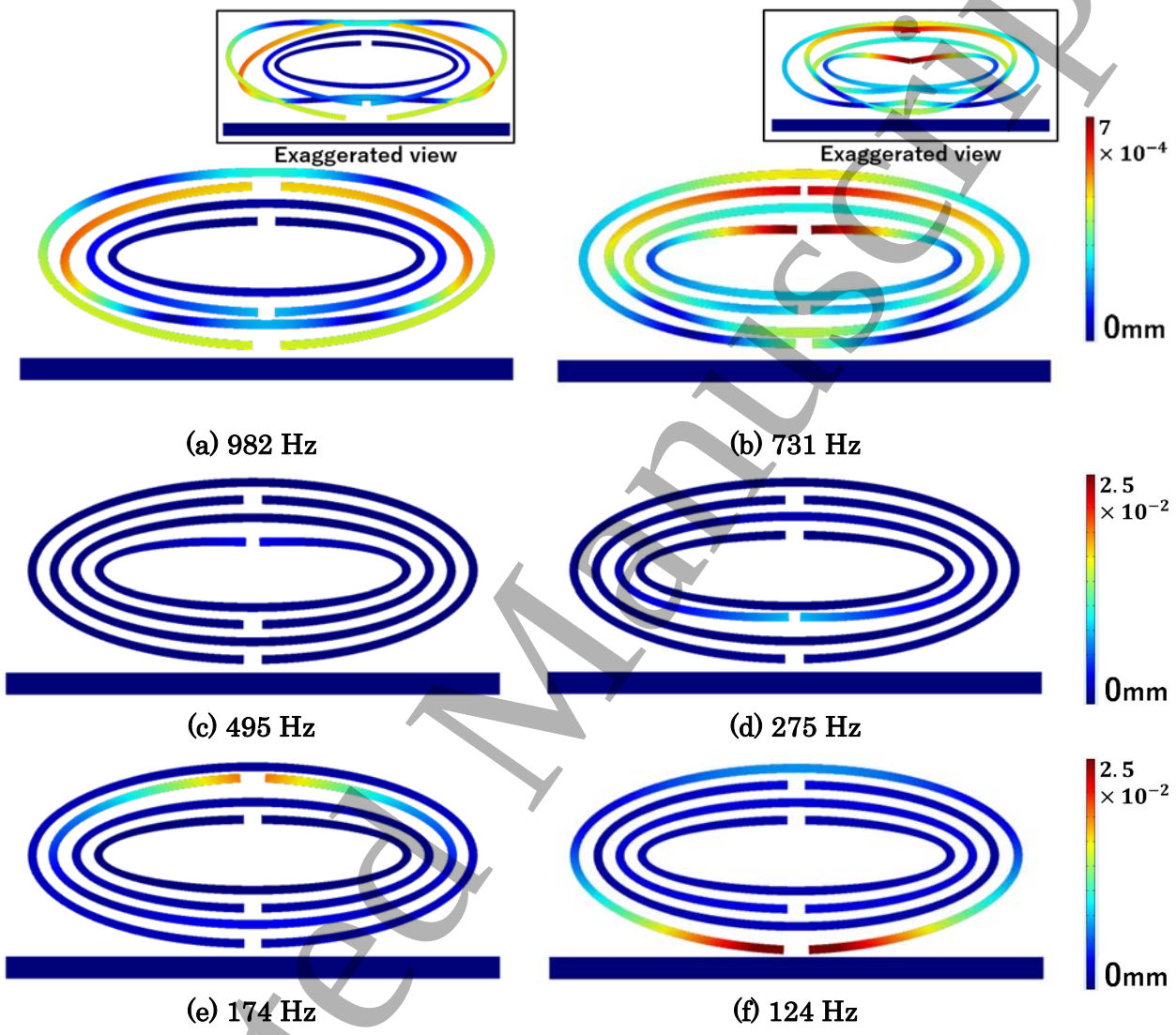

Figure 8 The mode shape and displacement at (a) 982 Hz, (b) 731 Hz, (c) 495 Hz, (d) 275 Hz, (e) 174 Hz, and (f) 124 Hz of the four-layer split tube. The color bar represents scales of the displacement norms drawn in the structure. The insets in (a) and (b) are exaggerated views of each mode shape, shown to emphasize participation of different harmonic modes.

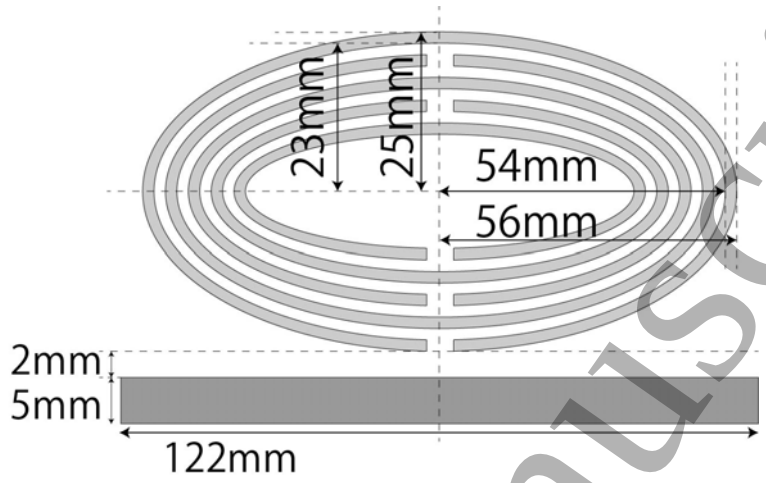

Figure 9 The cross-sectional view of a five-layer split tube.

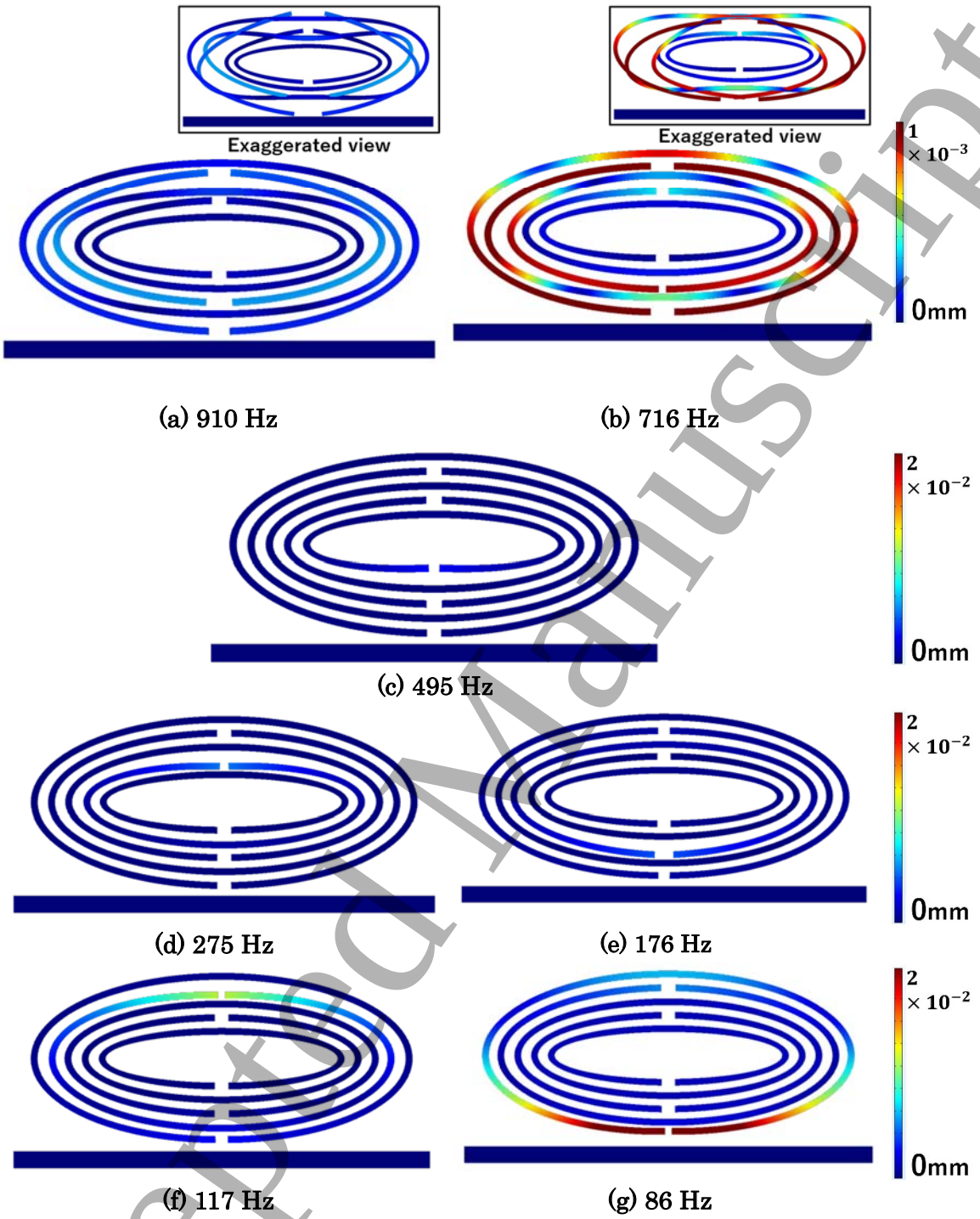

Figure 10 The mode shape and displacement at (a) 910 Hz, (b) 716 Hz, (c) 495 Hz, (d) 275 Hz, (e) 176 Hz, (f) 117 Hz, and (g) 86 Hz of the five-layer split tube. The color bar represents scales of the displacement norms drawn in the structure. The insets in (a) and (b) are exaggerated views of each mode shape, shown to emphasize participation of different harmonic modes.

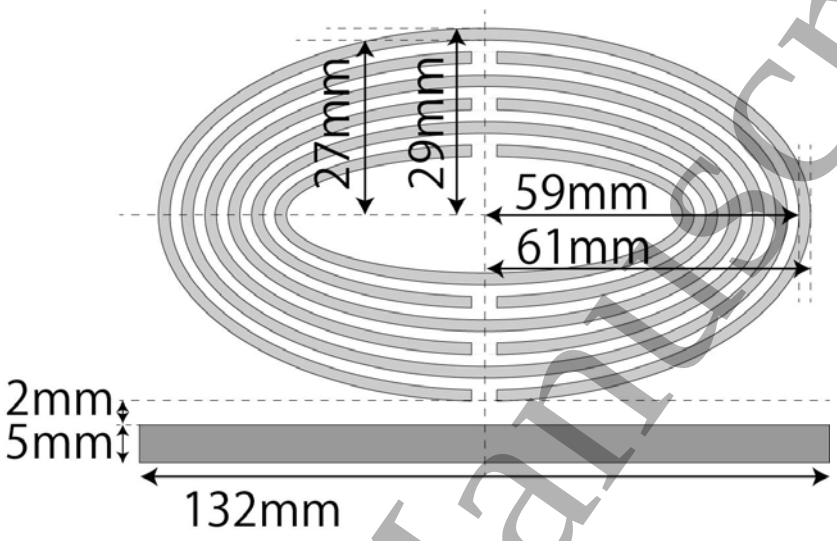

Figure 11 The cross-sectional view of a six-layer split tube.

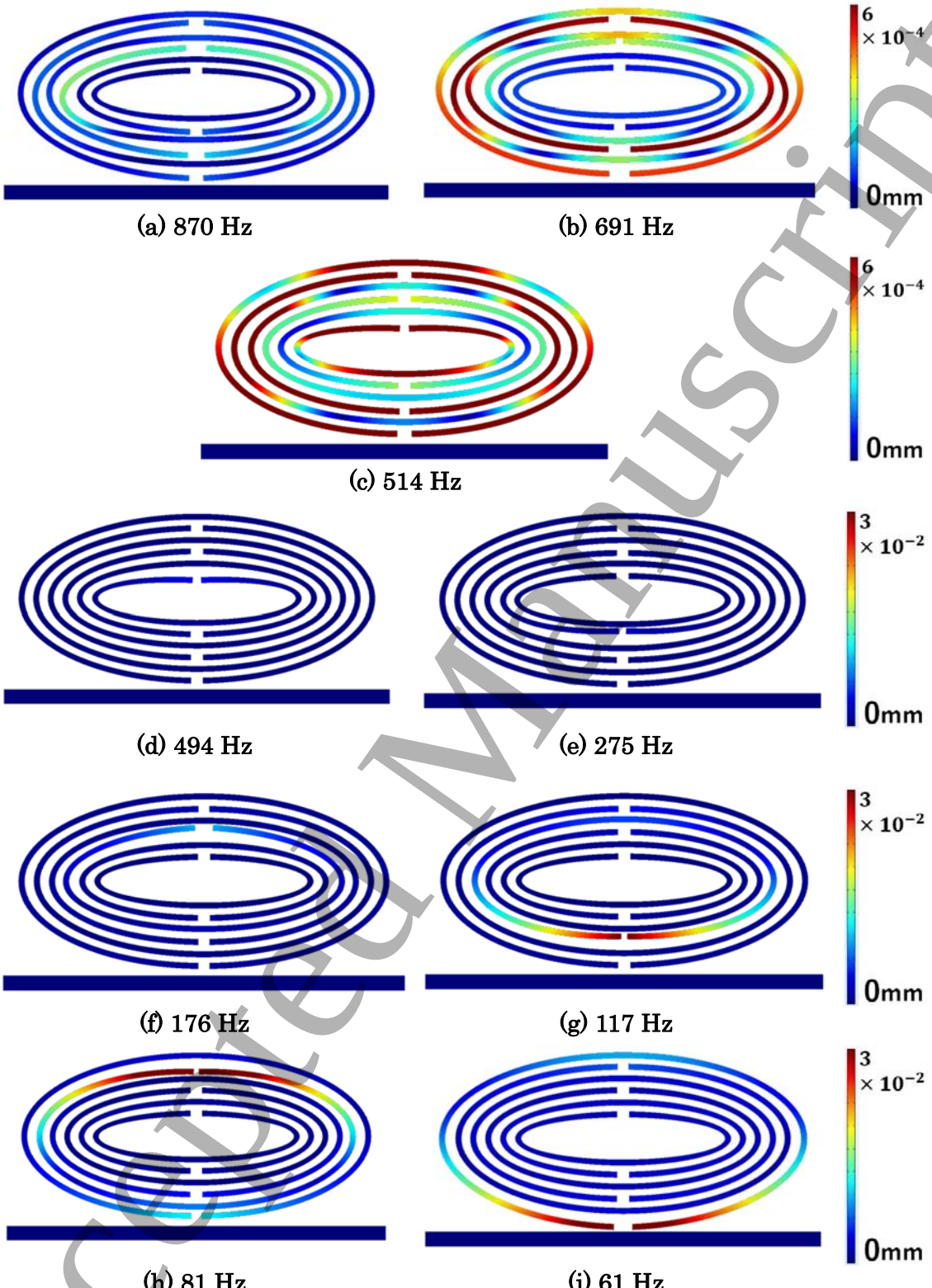

Figure 12 The mode shape and displacement at (a) 870 Hz, (b) 691 Hz, (c) 514 Hz, (d) 494 Hz, (e) 275 Hz, (f) 176 Hz, (g) 117 Hz, (h) 81 Hz, and (i) 61 Hz of the six-layer split tube. The color bar represents scales of the displacement norms drawn in the structure.